The BMTV triangle plane-filling curve

Herman Haverkort, 20 November 2022

In 2012, Ventrella [1] published a plane-filling curve that is unusual in that its approximating curves cannot be drawn on a regular grid. The curve seemed to fill some kind of fractal shape (see Figure 1) in such a way that it contains self-similar parts in infinitely many orientations. In 2017, this was proven by Bandt, Mekhontsev and Tetenov [2], using powerful mathematical and computational tools. In the honour of these four authors, I will call the shape that is filled the BMTV triangle.

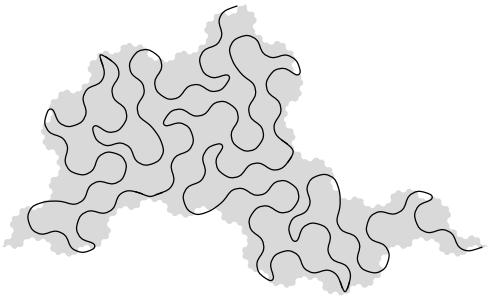

Figure 1: The mysterious plane-filling curve.

Now that it is known what this fractal shape looks like, one may wonder: is there a more direct way to describe this fractal shape and thus understand the plane-filling character of Ventrella's curve? I have been trying to describe the underlying tessellation with the approach of my note on the Rauzy triangle curve [3], where I start with a simple shape and describe how to refine its boundary and its subdivision into tiles simultaneously. However, for the BMTV triangle, it seems we have to describe its boundary first, and then the tessellation.

Below is my description of the BMTV triangle plane-filling curve. Note that this description cannot replace the work by Bandt et al. and Ventrella. I do not describe how to find such curves and I do not describe how to find a proof that they fill the plane—as Bandt et al. did. I will just give a description of this particular curve in hindsight, which may serve as a verification of the results by Bandt et al.

The boundary of the BMTV triangle consists of fractal curves that can be described by the following L-system. We define the following symbols:
b_k: move forward over a distance $1/(\sqrt{5})^k$;
w_k: move forward over a distance $\sqrt{2}/(\sqrt{5})^k$;
l_x: turn left by an angle of $\arctan(1/x)$;
r_x: turn right by an angle of $\arctan(1/x)$.
Graphically, we represent b_k and w_k by black and write arrows, respectively. For x in l_x and r_x we use values from $\{-1, 0, 1, 2, 3, 7\}$, where -1 denotes a 135 degrees' turn, 0 denotes a 90 degrees' turn, and the remaining values produce turns of approximately 45, 26.57, 18.43, and 8.13 degrees, respectively. Note that a sequence $l_2 l_3$ has the same effect as l_1, while $l_3 l_7$ is effectively l_2.

For a sequence (word) S that is composed of these symbols, let $\overline{S}$ represent a geometrically reflected version of S: it is obtained from S by replacing l_x by r_x and vice versa, and by replacing each other symbol y by $\overline{y}$ and vice versa. Furthermore, let $R(S)$ be the geometric reverse of S, that is, a representation of the same path traversed in the opposite direction. We obtain $R(S)$ from S by reversing the order of the symbols while replacing l_x by r_x and vice versa, and replacing each other symbol y by $R(y)$ and vice versa.

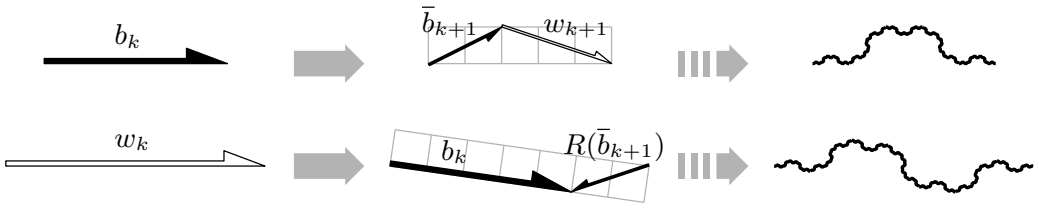

Figure 2: Production rules and limit curve for b_k (top) and w_k (bottom), with grids added to clarify the tangents of the turn angles.

The symbols b_k and w_k each represent a curve section that is recursively described by the following production (substitution) rules (see Figure 2):

$$\begin{aligned} b_k &\rightarrow l_2\ \overline{b}_{k+1}\ r_2 r_3\ w_{k+1}\ l_3; \\ w_k &\rightarrow r_7\ b_k\ l_2\ R(\overline{b}_{k+1})\ r_2 l_7. \end{aligned}$$

Note that in each production rule, the substitute (the right-hand side) ends with a turn, so that a turtle that woud interpret the substitute ends in the same state (position and orientation) as when it would interpret the substituted symbol (the left-hand side) directly.

If we start with a sequence that consists of only b_k or w_k (for any k) and apply the production rules repeatedly, the curve that is described by the sequence converges to a fractal curve; see the sketch in Figure 2. Henceforth we will equate any sequence S with the limit curve that results from continued application of the production rules to the symbols that make up S. The symmetries of the curves b_k and w_k are immediately apparent from the figure: $b_k = R(\overline{b}_k)$, that is, b_k is mirror-symmetric in the perpendicular bisector of its endpoints, whereas $w_k = R(w_k)$, that is, w_k is centrally symmetric. This can also be proven from the production rules, as follows.

$w_k = R(w_k)$: From the production rules we get:

$$w_k = r_7\ b_k\ l_2\ R(\overline{b}_{k+1})\ r_2 l_7 = r_7 l_2\ \overline{b}_{k+1}\ r_2 r_3\ w_{k+1}\ l_3 l_2\ R(\overline{b}_{k+1})\ r_2 l_7. \tag{1}$$

The leading part, before w_{k+1}, is thus the same as the reverse of the trailing part, after w_{k+1}. The symmetry of w_k, expanded until the sizes of the segments drop below a fixed threshold, can now be proven by induction on decreasing k. Thus, in the limit as the size threshold approaches zero, w_k is symmetric as well. To put it differently: if we keep expanding w as in Equation 1, then the leading and the trailing part will continue to be each other's reverse, while the middle part shrinks to a point—thus proving the observed symmetry of the curve. Likewise, $\overline{w}_k = R(\overline{w}_k)$.

$b_k = R(\overline{b}_k)$: From the production rules and the symmetry of w_{k+1} we get:

$$\begin{array}{lcl} b_k & = & R(\overline{b}_k) \quad \Leftrightarrow \\ l_2\ \overline{b}_{k+1}\ r_2 r_3\ w_{k+1}\ l_3 & = & l_3\ R(\overline{w}_{k+1})\ r_3 r_2\ R(b_{k+1})\ l_2 \quad \Leftrightarrow \\ l_2\ \overline{b}_{k+1}\ r_2 r_3\ R(w_{k+1})\ l_3 & = & l_3\ \overline{w}_{k+1}\ r_3 r_2\ R(b_{k+1})\ l_2 \quad \Leftrightarrow \\ l_2\ \overline{b}_{k+1}\ r_2 r_3 r_7 l_2\ \overline{b}_{k+2}\ r_2\ R(b_{k+1})\ l_7 l_3 & = & l_3 l_7\ \overline{b}_{k+1}\ r_2\ R(b_{k+2})\ l_2 r_7 r_3 r_2\ R(b_{k+1})\ l_2 \quad \Leftrightarrow \\ l_2\ \overline{b}_{k+1}\ r_2\ \overline{b}_{k+2}\ r_2\ R(b_{k+1})\ l_2 & = & l_2\ \overline{b}_{k+1}\ r_2\ R(b_{k+2})\ r_2\ R(b_{k+1})\ l_2 \quad \Leftrightarrow \\ \overline{b}_{k+2} & = & R(b_{k+2}). \end{array}$$

The second step exploits the symmetry of w_{k+1}, and the fourth step follows from rewriting the turns. Again, the proof can be completed by induction or by continued expansion of the middle terms on the second-last line.

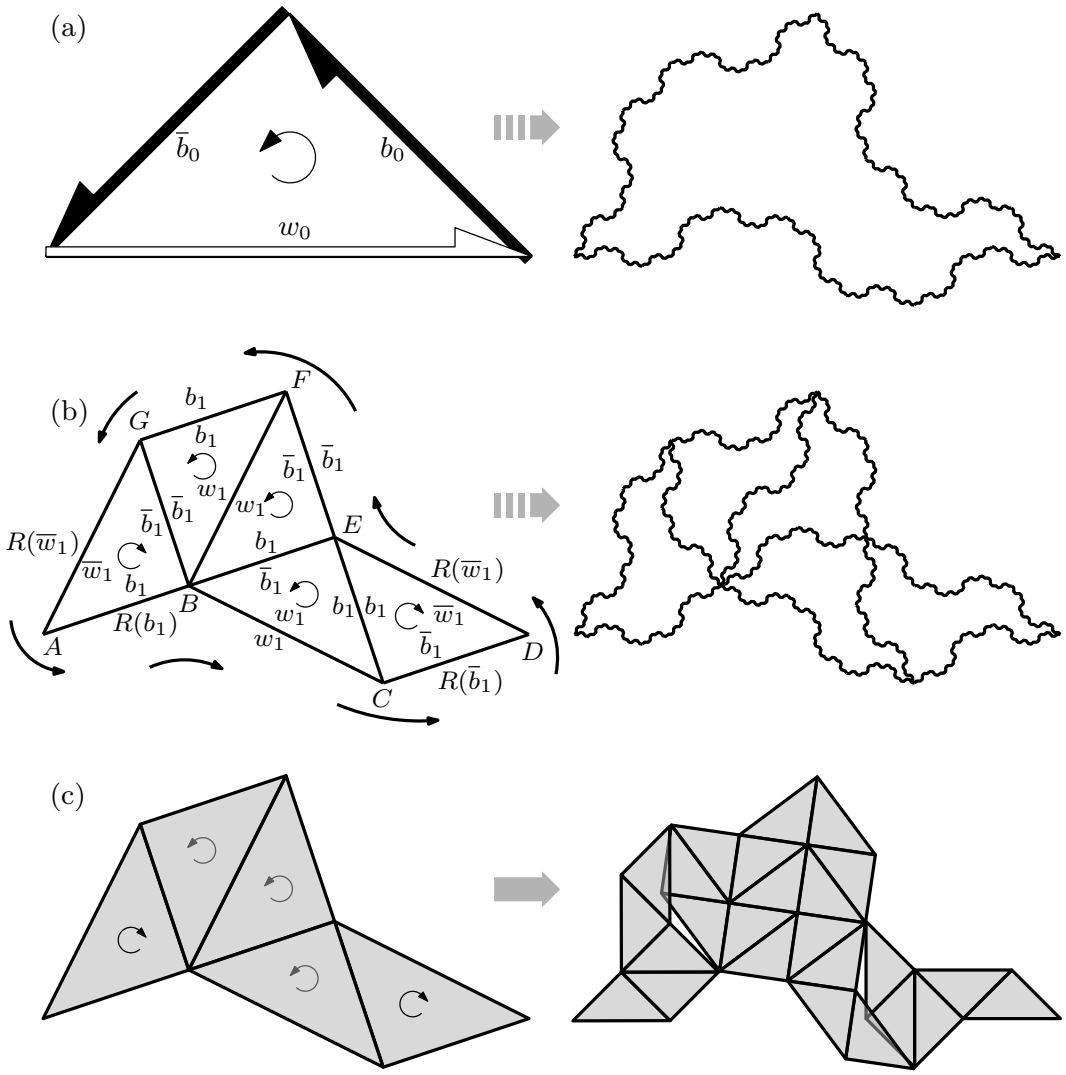

Figure 3: (a) The shape of the tiles. (b) Top-level tessellation and skeletton of the plane-filling curve. (c) In recursion, the approximating triangles do not tile the plane.

The complete boundary of the BMTV triangle is now given by the closed curve $w_0\ l_{-1}\ b_0\ l_0\ \overline{b}_0\ l_{-1}$: see Figure 3(a) for a sketch before expansion and a sketch after full expansion. Using the substitutions, symmetries and turn rewriting rules given above, we can rewrite the boundary as:

$$
\begin{array}{cccccccccccccc}
 & & w_0 & & l_{-1} & & b_0 & & l_0 & & \overline{b}_0 & & l_{-1} = \\
 & & w_0 & & l_{-1} & & R(\overline{b}_0) & & l_0 & & \overline{b}_0 & & l_{-1} = \\
r_7 & & b_0 & & l_2\ R(\overline{b}_1) & & r_2 l_7 l_{-1} l_3 & R(\overline{w}_1) & r_3 r_2 & R(b_1) & l_2 l_0 r_2 & b_1\ l_2 l_3 & \overline{w}_1 & r_3 l_{-1} = \\
r_7 l_2 & \overline{b}_1 & r_2 r_3 & w_1\ l_3 l_2 & R(\overline{b}_1) & & r_2 l_7 l_{-1} l_3 & R(\overline{w}_1) & r_3 r_2 & R(b_1) & l_2 l_0 r_2 & b_1\ l_2 l_3 & \overline{w}_1 & r_3 l_{-1} = \\
l_3 & R(b_1) & r_1 & w_1\ l_1 & R(\overline{b}_1) & & l_{-1} & R(\overline{w}_1) & r_1 & \overline{b}_1 & l_0 & b_1\ l_1 & R(\overline{w}_1) & l_{-1} r_3,
\end{array}
$$

and we can subdivide the triangle into five tiles as in Figure 3(b).

From this figure one might get the impression that on each level of recursion, a tessellation with equilateral right triangles can serve as an approximation of the true tessellation. However, as Figure 3(c) shows, this is not quite true. One could say that the tiles ABG and CDE are to blame for this, since they are reflected as compared to the others. In contrast, in most published fractal tilings, all tiles are reflected, or none of them, but not just some. As a result of the reflections, the tile boundaries BG and CE are approximated in different ways from the left and from the right.

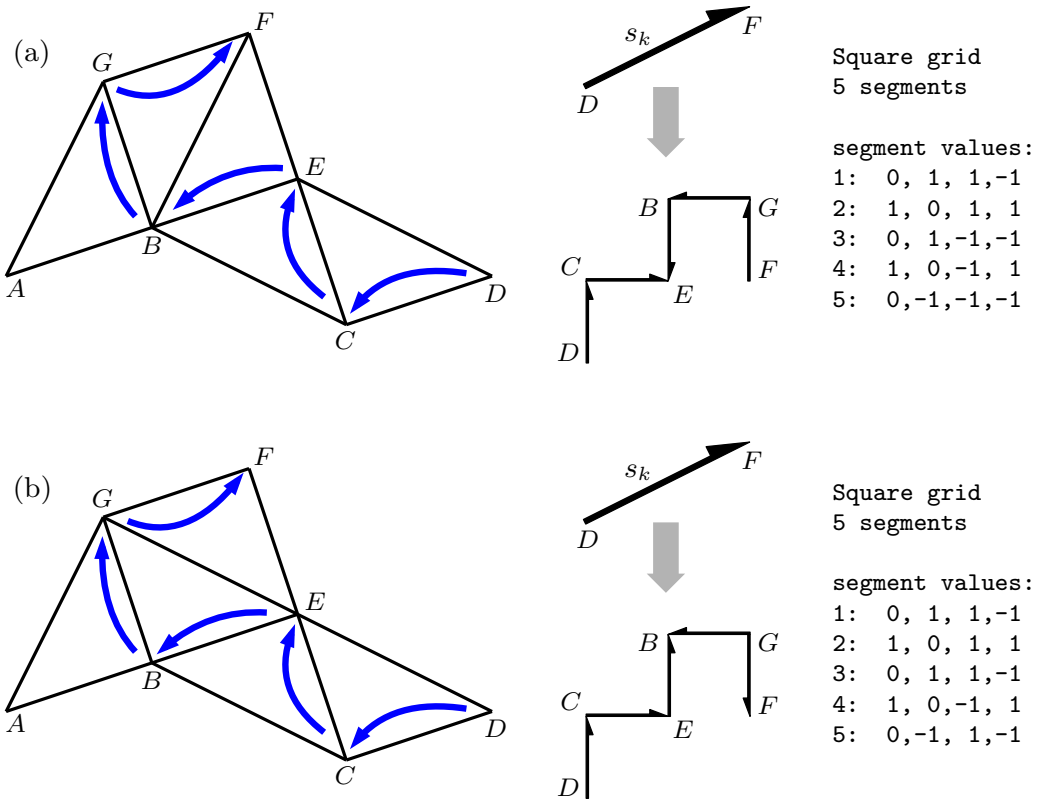

Figure 4: Generator and definition of the plane-filling curve in Ventrella's notation (from [1]). in this notation, $i : x, y, r, m$ means that the vector from the starting point to the end point of the i-th segment of the plane-filling curve is (x, y), where $r = -1$ or $r = 1$ indicates whether the segment represents a reversed or a forward copy, respectively, of the scaled, rotated and translated curve as a whole; $mr = -1$ or $mr = 1$ indicates whether the segment is reflected or not, respectively.

Nevertheless, as Figure 3(b) shows, the tessellation works out in the end, thanks to the symmetries in the fractal boundary curves. The edges of the tiles match the corresponding parts of the boundary of the complete shape: where matching parts are described from the same direction (counterclockwise on the outside, counterclockwise on the inside, as with BC, EF and FG) they are given by equal symbols; where matching parts are described in opposite directions (counterclockwise on the outside, clockwise on the inside, as with AB, CD, DE and GA), the corresponding symbols are indeed each other's geometric reverse. Similarly, where edges between tiles are labelled in the same direction from both sides (GB and CE) they are labelled with the same symbol from both sides; where they are labelled in opposite directions (BF and BE), the symbols are each other's geometric reverse (recall that $w_1 = R(w_1)$ and $b_1 = R(\overline{b}_1)$).

A plane-filling curve for the BMTV triangle is now obvious and is sketched by the blue curves in Figure 4(a). It is given by the following production rule starting from the edge $s_0 = DF$ (see also Figure 4):

$$s_k \to l_3 l_1 \ \overline{s}_{k+1} \ r_0 \ s_{k+1} \ l_0 \ R(s_{k+1}) \ r_0 \ R(\overline{s}_{k+1}) \ r_0 \ R(s_{k+1}) \ l_2 l_0.$$

As Bandt et al. and Ventrella observed, another tessellation and corresponding plane-filling curve can be obtained by reflecting the "square" $BEFG$, as in Figure 4(b).

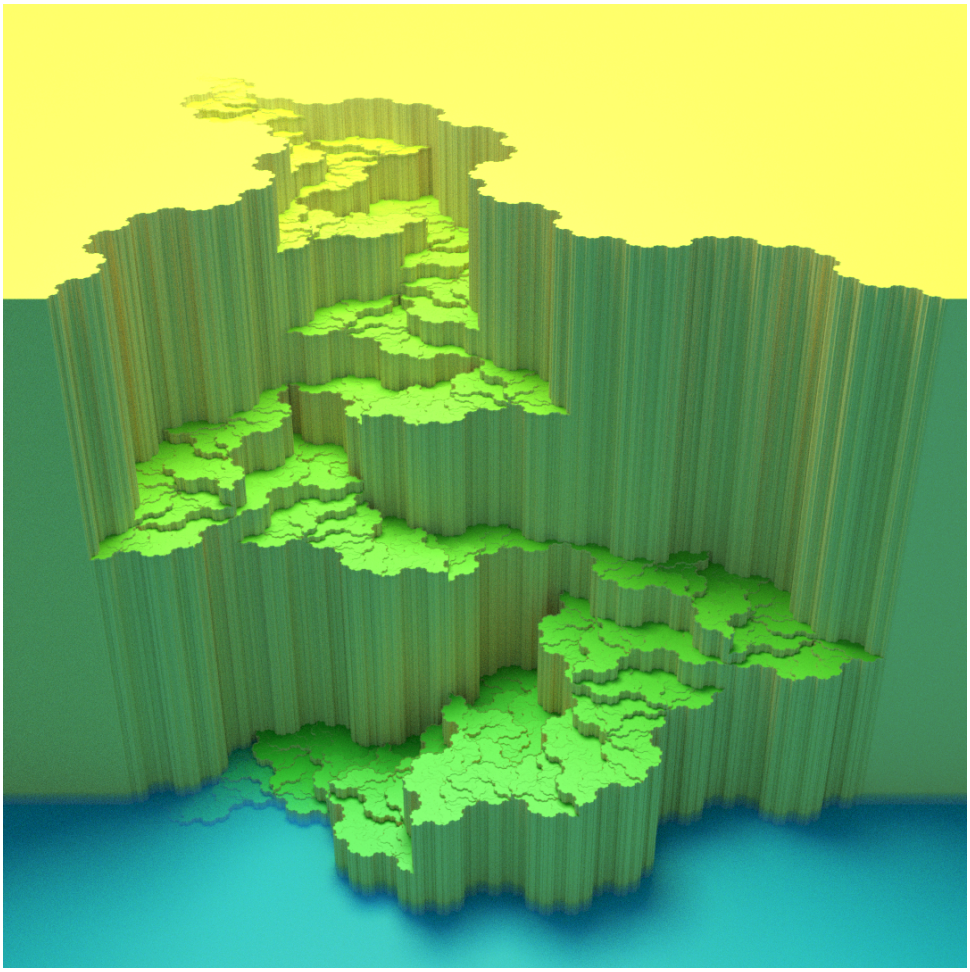

Figure 5: The BMTV triangle-filling curve visualised as an descending path by pftrail [4].

References

[1] Jeffrey Ventrella: *Brain-filling curves—A fractal bestiary.* Eyebrain Books, 2012.

[2] Christoph Bandt, Dmitry Mekhontsev and Andrei Tetenov: A single fractal pinwheel tile, in *Proc. Amer. Math. Soc.* 146:1271–1285, 2018.

[3] Herman Haverkort: *The Rauzy triangle plane-filling curve.* Manuscript on http://spacefillingcurves.net, 2022.

[4] Herman Haverkort: Plane-filling trails, in Proc. *Symp. on Comp. Geom. Media Exposition 2020*, LIPIcs 164:81:1–5; full version at *CoRR*, `https://arxiv.org/abs/2003.12745`.